Molecular-weight distributions in the miniemulsion polymerization of styrene initiated by oil-soluble initiators

Juan A. Alduncin and José M. Asua*

Grupo de Ingeniería Química, Departamento de Química Aplicada, Facultad de Ciencias Químicas, Universidad del País Vasco, Apdo. 1072, 20080 San Sebastián, Spain

(Received 9 November 1993; revised 18 February 1994)

The evolution of the molecular-weight distributions in the batch miniemulsion polymerization of styrene initiated by different oil-soluble initiators (lauroyl peroxide, benzoyl peroxide and azobisisobutyronitrile) was investigated. Two series of polymerizations were carried out. In the first, miniemulsions contained only oil-soluble initiators to minimize monomer droplet degradation by molecular diffusion. In the second, the stability of the monomer droplets was reinforced with hexadecane. Also, a series of conventional emulsion polymerizations were carried out. The effect of both the type of initiator and the extent of the compartmentalization of initiator radicals between the polymer particles on the molecular-weight distributions were analysed by means of a mathematical model. A good agreement between experimental results and model predictions was achieved.

(Keywords: molecular-weight distribution; miniemulsion polymerization; oil-soluble initiator)

INTRODUCTION

Miniemulsions are finely divided oil-in-water dispersions stabilized against coagulation by a conventional emulsifier (usually an anionic emulsifier) and containing a highly water-insoluble compound such as a fatty alcohol or a long-chain alkane to minimize the Ostwald ripening effect, namely, the diffusion of oil phase from small to large droplets to minimize the interfacial free energy of the system. Ugelstad *et al.*[1] showed that monomer miniemulsions polymerize in a distinct way because particle nucleation occurred in submicrometre monomer droplets. This nucleation mechanism leads to a broad particle size distribution[2]. This characteristic can be used to produce high-solids-content (65 wt%) latexes of low viscosity[3]. Another advantage of this process is that miniemulsion polymerizations in continuous stirred tank reactors (CSTR) do not show the oscillatory behaviour characteristic of conventional emulsion polymerization in CSTR[4]. The difference was attributed to the different nucleation mechanisms: nucleation in monomer droplets for the miniemulsion polymerization, and micellar and homogeneous nucleation for the conventional emulsion polymerization. A drawback of the miniemulsion polymerization is that the water-insoluble compound remains in the polymer particles after polymerization and may have a deleterious effect on the properties of the polymer. Alduncin *et al.*[5] explored the possibility of replacing the highly water-insoluble compound with initiators of different water solubilities. The authors reported that miniemulsion polymerizations carried out with lauroyl peroxide (LPO) led to a broad particle size distribution similar to that of the miniemulsion polymerization carried out with hexadecane. On the other hand, more water-soluble initiators such as benzoyl peroxide (BPO) and azobisisobutyronitrile (AIBN) were not water-insoluble enough to avoid the Ostwald ripening effect and extensive monomer droplet degradation occurred.

In the present work, the effect of the type of oil-soluble initiator on the evolution of the molecular-weight distribution (*MWD*) obtained in the batch miniemulsion polymerization of styrene was studied. In addition, comparison with the *MWD* obtained in other series of experiments where the stability of the monomer droplets was assured by using hexadecane (HD) in addition to the oil-soluble initiator was performed.

EXPERIMENTAL

Styrene was distilled under reduced pressure and stored at −18°C until use. Distilled and deionized water (DDI) was used throughout the work. The other materials were used as received. The emulsifier used was sodium lauryl sulfate (SLS) (Merck) 90%, the remaining 10% being mainly inorganic salts. Azobisisobutyronitrile (AIBN) (Merck), benzoyl peroxide (BPO) (Merck) and lauroyl peroxide (LPO) (Fluka) were used as oil-soluble initiators. The water solubilities of these initiators are given in *Table 1*. *Table 2* summarizes the three series of polymerizations carried out using the recipes given in *Table 3*. The first series comprised polymerizations of miniemulsions containing initiators of different water solubility but no HD. These polymerizations were carried out at 75°C in a 1 litre glass unbaffled jacketed reactor equipped with a reflux condenser, stainless-steel stirrer

* To whom correspondence should be addressed

0032-3861/94/17/3758–08

Table 1 Values of the parameters used in the calculations[a]

	LPO	BPO	AIBN
Water solubility (g/100 g H_2O)	2×10^{-9} (ref. 7)	3×10^{-4} (ref. 7)	0.04 (ref. 6)
k_I (s^{-1})	1×10^{-4} (ref. 8)	1.83×10^{-5} (ref. 8)	9.25×10^{-5} (ref. 9)
C_I	0.024 (ref. 10)	0.16[b]	0.05[c]

$k_p = 4.13 \times 10^5$ cm^3 mol^{-1} s^{-1} (ref. 11)	$C_M = 1.6 \times 10^{-4}$ (ref. 12)
$k_{t0} = 1.11 \times 10^4$ cm^3 mol^{-1} s^{-1} (ref. 16)	$k_{tw} = k_{t0}$
$f = 0.6$	$F = 10^{-3}$
$D_w = 10^{-5}$ cm^2 s^{-1}	$D_p = 10^{-6}$ cm^2 s^{-1}
$m_d = 2400$	

[a] Parameters are defined in the text. In addition, D_p and D_w are diffusion coefficients in the polymer particles and in the aqueous phase, respectively; F is the radical capture efficienty; k_{t0} and k_{tw} are termination rate constants at zero polymer content and in the aqueous phase, respectively; and m_d is the monomer partition coefficient between the polymer particles and the aqueous phase
[b] Value estimated to fit the experimental data; literature value 0.1 (ref. 10)
[c] Value estimated to fit the experimental data; literature value 0.09 (ref. 10)

Table 2 Summary of the polymerizations carried out

Run	Initiator	HD	Sonication
1	LPO	No	Yes
2	BPO	No	Yes
3	AIBN	No	Yes
4	LPO	Yes	Yes
5	BPO	Yes	Yes
6	AIBN	Yes	Yes
7	LPO	No	No
8	BPO	No	No
9	AIBN	No	No

Table 3 Recipes used in the polymerizations, $T = 75°C$

	Miniemulsion polymerizations	'Classical' miniemulsion polymerizations	Conventional emulsion polymerizations
Styrene (g)	144.6	144.6	144.6
Sodium lauryl sulfate (g)	1.237	1.237	1.237
Initiator (g)	3.624	3.624	3.624
Hexadecane (g)	–	3.289	–
DDI water (g)	455.2	455.2	455.2

	Concentrations of initiators and hexadecane in momomer phase	
	g/100 g monomer	mol/l
Lauroyl peroxide	2.44	0.0556
Benzoyl peroxide	2.44	0.0914
AIBN	2.44	0.1349
Hexadecane	2.17	0.0980

(stirrer speed 200 rev min^{-1}), nitrogen inlet and sampling device. For the oil-soluble initiators, the miniemulsions were made by first mixing a solution of emulsifier in water with another of initiator in monomer. Then, the system was subjected to sonication (Branson Sonifier 450) at room temperature under agitation provided by a magnetic bar stirrer. The conditions for the sonication were as follows: output control, 8; duty cycle, 80%; sonication time, 2 min. In the second series, the miniemulsion polymerizations were carried out using the same procedure as in the previous series but including hexadecane (HD), in addition to the initiator (*Table 3*). These miniemulsion polymerizations will be denoted as

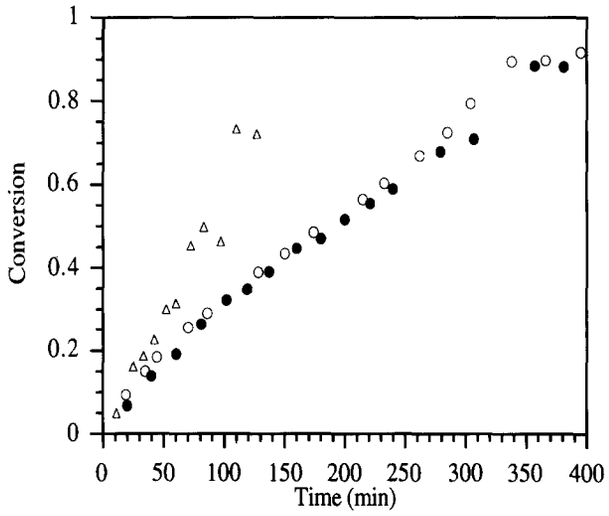

Figure 1 Time evolution of the conversion in the polymerizations initiated by LPO: (○) miniemulsion polymerization; (●) 'classical' miniemulsion polymerization; (△) conventional emulsion polymerization

'classical' miniemulsion polymerizations. In the third series, conventional emulsion polymerizations were carried out, namely, neither HD nor sonication were used. In all experiments, samples were withdrawn during the process and the polymerization was stopped-short with hydroquinone. The conversion was determined by gravimetry and the particle size was measured by transmission electron microscopy (TEM). Particle size distribution (*PSD*) was determined by means of a graphics tablet (Summasketch Plus). Molecular-weight distributions were obtained by g.p.c. using 2 PL 20 μ Mixed A columns from Polymer Laboratories and a refractive-index detector. The solvent was tetrahydrofuran, flow rate 1 cm^3 min^{-1} and injection volume 0.1 cm^3. The columns were calibrated with nine standard polystyrene samples.

RESULTS AND DISCUSSION

Figure 1 presents the evolution of the conversion in the polymerizations initiated by LPO. It can be seen that, within the experimental error, polymerization rate was not affected by the presence of HD in the miniemulsion recipe. The increase of the polymerization rates after 65% conversion can be attributed to the gel effect. The

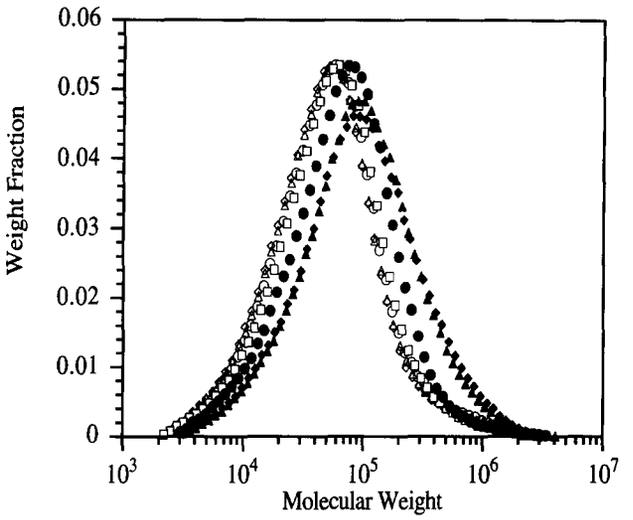

Figure 2 Evolution of the molecular-weight distribution in the miniemulsion polymerization initiated by LPO: (○) $x=0.09$; (△) $x=0.18$; (◇) $x=0.29$; (□) $x=0.43$; (●) $x=0.60$; (▲) $x=0.79$; (◆) $x=0.92$

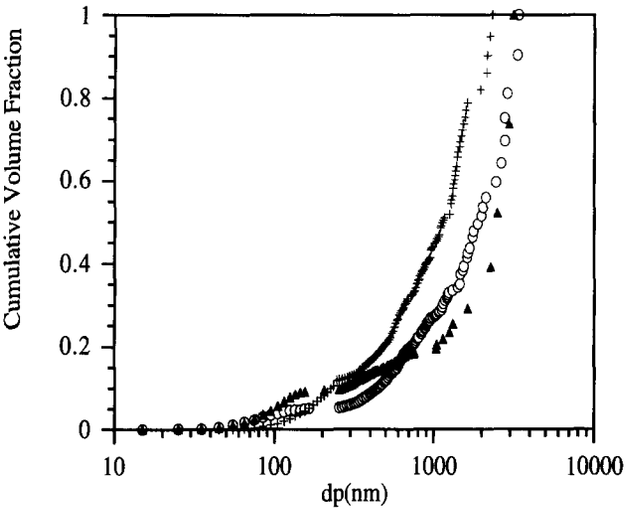

Figure 3 Cumulative particle volume distributions in the miniemulsion polymerizations initiated by LPO: (○) $x=0.26$; (▲) $x=0.43$; (+) $x=0.92$

conventional emulsion polymerization could not be completed because extensive coagulation occurred. It was found that the coagulum accounted for the 81 wt% of polymer in the reactor.

Figure 2 presents the evolution of the *MWD* during the miniemulsion polymerization initiated by LPO. It can be seen that molecular weight remained roughly constant at the beginning of the process and increased significantly after conversion $x=0.6$ due to the gel effect. The average molecular weights of these samples, which ranged from 28 000 to 50 000 for M_n and from 90 000 to 170 000 for M_w, are typical of bulk polymerization. This means that there is not a significant influence of compartmentalization of initiator radicals between the particles on the molecular weights. (The compartmentalization of initiator radicals between the particles will be referred to simply as compartmentalization throughout this paper.) Therefore, polymerization should proceed under Smith–Ewart case 3 conditions, i.e. with number of radicals per particle $\bar{n} \gg 0.5$. For styrene, this means that polymerization occurred preferentially in large polymer particles. *Figure 3* presents the evolution of cumulative particle volume distribution for the miniemulsion polymerization initiated by LPO. It can be seen that most of the polymer phase was in particles larger than 500 nm in diameter where bulk-like polymerization is expected to occur.

In order to verify these hypotheses, the dependence of n on the particle size was calculated by means of the approach proposed by Asua *et al.*[14] using the parameters in *Table 1*. The monomer concentration in the polymer particles was assumed to be that of equilibrium swelling in a conventional emulsion polymerization[15] and the termination rate coefficient, k_t, was calculated by means of the following equation[13]:

$$k_t = k_{t0}\{\exp[-(0.8126x_e + 3.4352x_e^2 - 0.2982x_e^3)]\}^2 \quad (1)$$

where a value of $x_e=0.4$ (apparent conversion in the polymer particles at equilibrium swelling) was assumed.

Figure 4 presents the results of the calculation of n. It can be seen that, for particle diameter $d_p > 300$ nm, $n \gg 0.5$, namely the model predicted that compartmentalization was negligible for most of the polymer phase. This result is in agreement with the experimental findings.

The results presented above show that most of the polymerization occurred under bulk-like conditions. In a bulk polymerization, the instantaneous number-average molecular weight, M_n, can be calculated as follows:

$$\frac{1}{M_n} = \frac{1}{P_M}\left(\frac{(fk_lk_t[I])^{1/2}}{k_p[M]} + C_M + C_I\frac{[I]}{[M]}\right) \quad (2)$$

where P_M is the monomer molecular weight, f the efficiency factor for initiator decomposition, k_l the rate constant for initiator decomposition, k_t the termination rate constant, [I] the initiator concentration, k_p the propagation rate constant, [M] the monomer concentration, C_M the monomer chain-transfer constant, and C_I the initiator chain-transfer constant. The cumulative number-average molecular weight is given by:

$$\bar{M}_n = \frac{x}{\int_0^x (1/M_n)\,dx} \quad (3)$$

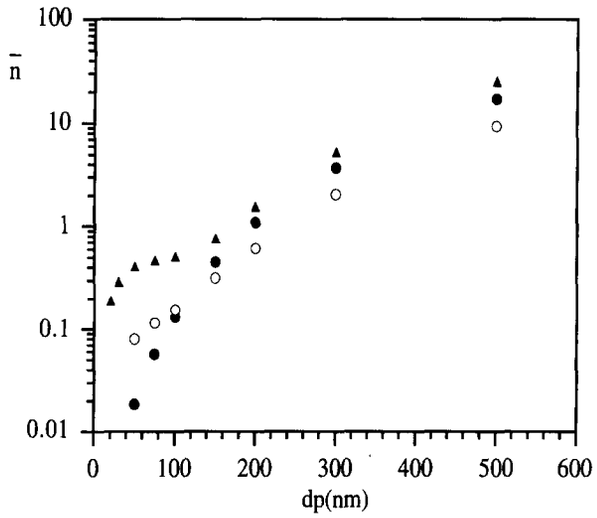

Figure 4 Effect of the particle size on the average number of radicals per particle for the different oil-soluble initiators: (●) LPO; (○) BPO; (▲) AIBN

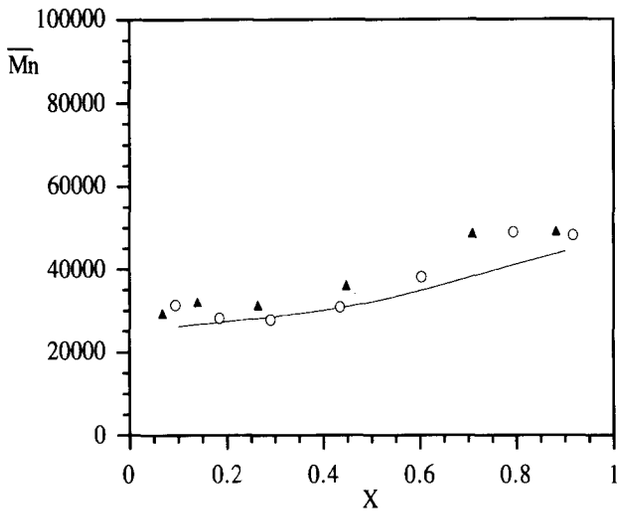

Figure 5 Comparison between experimental and calculated values of the cumulative number-average molecular weight for the LPO-initiated miniemulsions: (—) model calculations; (○) miniemulsion polymerization; (▲) 'classical' miniemulsion polymerizations

Equations (2) and (3) have been used in an attempt to simulate the evolution of the number-average molecular weight on the miniemulsion processes using the values of the parameters in *Table 1*. The initiator concentration was calculated as follows:

$$[I] = [I]_0 \exp(-k_i t) \quad (4)$$

where $[I]_0$ is the initial initiator concentration. As a first approximation, the monomer concentration was estimated by assuming that up to $x = 0.4$ the monomer concentration in the polymer particles is that of the equilibrium swelling in a conventional emulsion polymerization[15], and for $x > 0.4$ all of the monomer was in the latex particles:

$$x < 0.4 \qquad [M] = 5.26 \times 10^{-3} \text{ mol cm}^{-3} \quad (5)$$

$$x > 0.4 \qquad [M] = 5.26 \frac{(1-x)}{(1-0.4)} \text{ mol l}^{-1} \quad (6)$$

The termination rate constant was calculated using equation (1) with the following conditions:

$$x_e = 0.4 \qquad \text{for } x \leqslant 0.4$$

$$x_e = x \qquad \text{for } x \geqslant 0.4$$

Figure 5 presents a comparison between the experimental and calculated evolution of $\bar{M}_n$. It can be seen that a fairly good agreement was achieved. This further supports the conclusion that most of the polymerization occurred in large particles under bulk-like conditions, namely, compartmentalization was negligible. In the calculations of the $\bar{M}_n$ presented in *Figure 5*, it was assumed that LPO was uniformly distributed in the organic phase. However, due to the Ostwald ripening effect, monomer migrates through the aqueous phase to the larger polymer particles, whereas LPO likely remains in the small monomer droplets. Therefore, the polymerization in the large polymer particles would take place at a lower initiator concentration than is assumed and hence give polymer of a slightly higher $\bar{M}_n$. *Figure 5* shows some indications that this might be going on, but the extent of this effect cannot be quantified because droplet–particle coagulation (another possible phenomenon in mini-emulsion polymerization) may counteract it, bringing LPO to the large polymer particles.

Figure 6 presents the evolution of the *MWD* during the 'classical' miniemulsion polymerization initiated by LPO (run 2). It can be seen that this polymerization showed similar features to the miniemulsion polymerization initiated by LPO (run 1). In addition, the values of the cumulative number-average molecular weights were almost identical to those obtained in run 1 (see *Figure 5*).

Figure 7 presents a comparison between the *MWD* of the final samples of the polymerizations carried out with LPO. Two *MWD*s from the conventional emulsion process are included; one corresponds to the coagulum that accounted for 81 wt% of the polymer and the other to the latex. It can be seen that the *MWD*s of the miniemulsion polymerizations were close to that of the coagulated part of the conventional emulsion polymerization that presumably resulted from bulk polymerization. On the other hand, the *MWD* of the

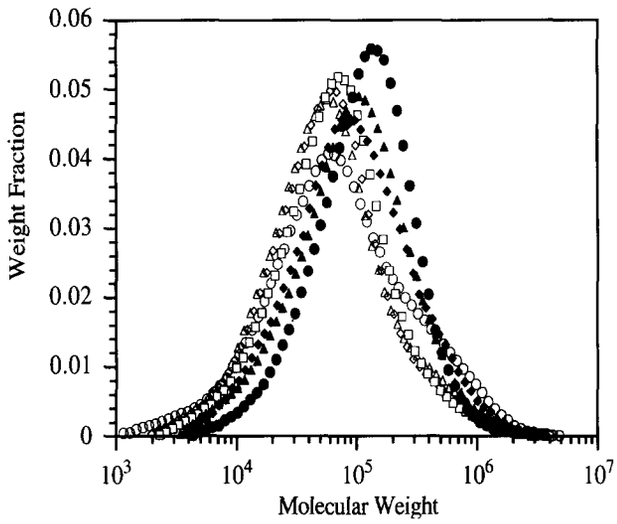

Figure 6 Evolution of the molecular-weight distribution in the 'classical' miniemulsion polymerization initiated by LPO: (○) $x = 0.07$; (△) $x = 0.14$; (◇) $x = 0.26$; (□) $x = 0.45$; (●) $x = 0.59$; (▲) $x = 0.71$; (◆) $x = 0.85$

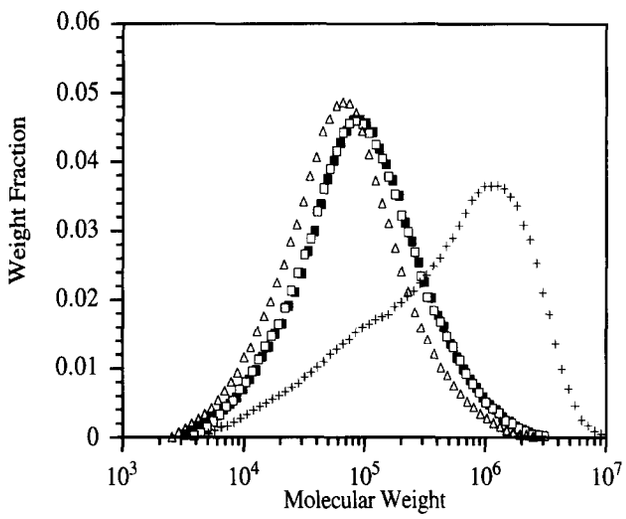

Figure 7 Comparison of the *MWD* of the final samples of the polymerizations carried out with LPO: (■) miniemulsion polymerization; (□) 'classical' miniemulsion polymerization; (△) coagulated fraction of the conventional emulsion polymerization; (+) non-coagulated fraction of the conventional emulsion polymerization

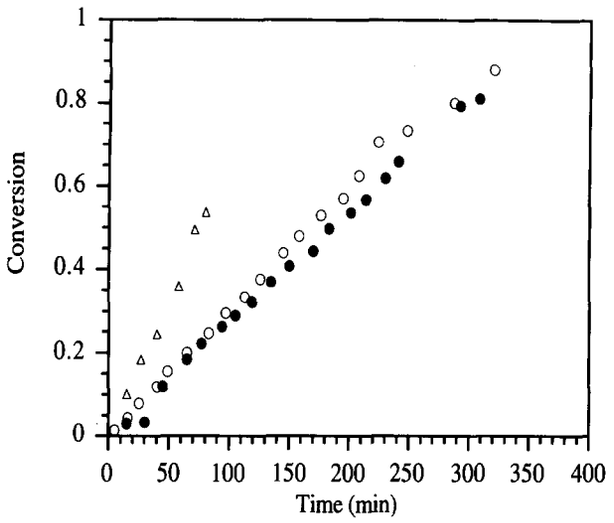

Figure 8 Time evolution of the conversion in the polymerizations initiated by BPO: (○) miniemulsion polymerization; (●) 'classical' miniemulsion polymerization; (△) conventional emulsion polymerization

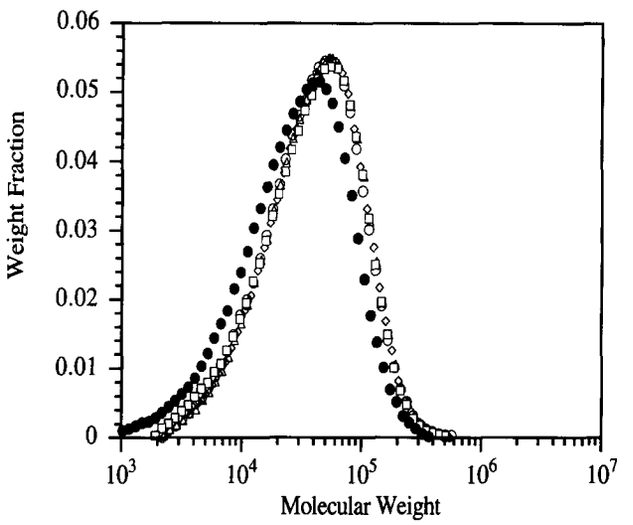

Figure 9 Evolution of the *MWD* in the miniemulsion polymerization initiated by BPO: (○) $x=0.08$; (△) $x=0.16$; (◇) $x=0.38$; (□) $x=0.53$; (●) $x=0.81$

non-coagulated part of the conventional emulsion polymerization showed a peak of high molecular weight characteristic of highly compartmentalized systems.

Figure 8 presents the time evolution of the polymerizations carried out with BPO, which is more water-soluble that LPO (see *Table 1*). It can be seen that the polymerization rate was not affected by the presence of HD during the first part of the polymerizations, but later, in the region where the gel effect was apparent, the polymerization rate of the miniemulsion polymerization was higher than that of the 'classical' miniemulsion process. Actually, *Figure 1* shows some indication that this behaviour also occurred in the LPO-initiated miniemulsions, but in that case differences were within experimental error. The lower polymerization rate in the 60% conversion region when HD was present might be due to the plasticizing effect of the HD that somehow delayed the onset of the gel effect. When the conventional emulsion polymerization was attempted, a large coagulum containing 78 wt% of the polymer was obtained.

Figure 9 presents the evolution of the molecular-weight distribution during the miniemulsion polymerization initiated by BPO. It can be seen that rather low molecular weights were obtained and that, in spite of the conversion–time curves showing a distinct gel effect, the molecular weight decreased during polymerization. This behaviour is also evident in the 'classical' miniemulsion polymerization (*Figure 10*). *Figure 11* presents the evolution of the cumulative particle volume distribution for the miniemulsion polymerizations initiated by BPO. It can be seen that most of the polymer phase was in particles larger than 500 nm in diameter. On the other hand, the calculations presented in *Figure 4* show that for such a system bulk-like conditions prevailed. The evolution of the cumulative number-average molecular weight was calculated by means of equations (2) and (3) using the parameters in *Table 1*. *Figure 12* shows that a fairly good agreement between experimental results and model predictions was achieved. According to the model, the decrease of the molecular weight in the gel effect

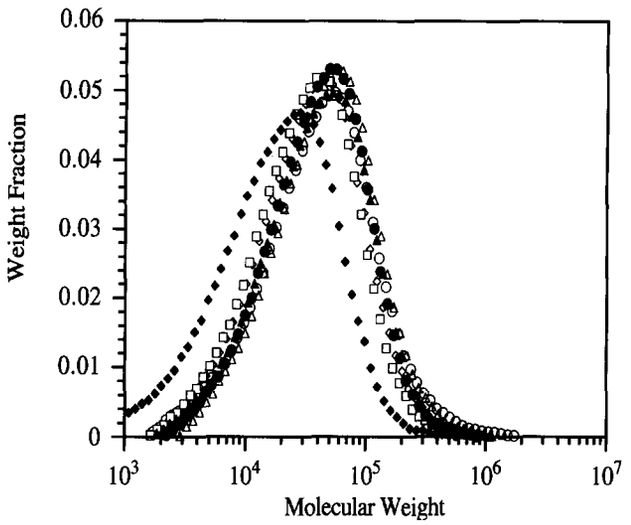

Figure 10 Evolution of the *MWD* in the 'classical' miniemulsion polymerization initiated by BPO: (○) $x=0.12$; (△) $x=0.18$; (◇) $x=0.26$; (□) $x=0.41$; (●) $x=0.57$; (▲) $x=0.64$; (◆) $x=0.81$

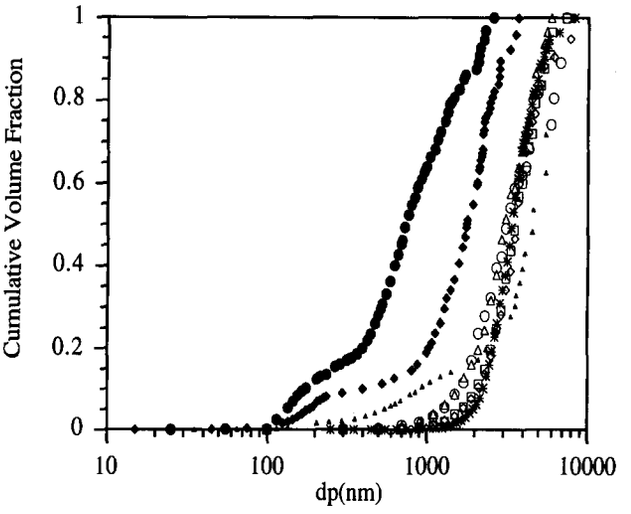

Figure 11 Cumulative particle volume distributions in the miniemulsion polymerizations initiated by BPO. Miniemulsion polymerization (run 2): (○) $x=0.12$; (△) $x=0.20$; (◇) $x=0.38$; (□) $x=0.63$; (*) $x=0.88$. 'Classical' miniemulsion polymerization (run 5): (●) $x=0.12$; (▲) $x=0.29$; (◆) $x=0.81$

region was due to chain transfer to the initiator that counteracted the influence of the gel effect. It has to be pointed out that an aspect not covered by the model is that the small initiator radicals may be mobile and capable of quick termination when the polymeric radicals are not.

Figure 13 presents a comparison between the *MWD* of the final samples of the polymerizations carried out with BPO. The molecular weights of the miniemulsion processes and that of the coagulum of the conventional emulsion polymerization were lower than that of the non-coagulated part of the conventional emulsion polymerization. In addition, comparison between *Figures 7* and *13* shows that the molecular weights obtained with BPO were lower than those obtained with LPO. According to the model, this difference was due to the different initiator chain-transfer constants.

Figure 14 presents the evolution of the conversion in the polymerizations initiated by AIBN. It can be seen that the polymerization rate for the 'classical' miniemulsion process was higher than that of the miniemulsion polymerization carried out without HD. This difference can be explained by the different compartmentalization of these systems. *Figure 15* presents the evolution of the cumulative particle volume distribution for these processes. It can be seen that, for the 'classical' miniemulsion polymerization (run 6), a significant part of the polymer phase was formed in small particles ($80\ \text{nm} < d_p < 200\ \text{nm}$), whereas in the absence of HD (run 3) most of the polymer was in large particles ($d_p > 1000$ nm). This difference was due to the presence of HD, which minimized the Ostwald ripening effect. *Figure 4* shows that, according to the model, substantial compartmentalization occurred for particles smaller than about 150 nm in diameter. An important consequence of the compartmentalization is that opportunities for the mutual termination of radicals are reduced relative to the case of a less compartmentalized system. Therefore, polymerization rate increased with compartmentalization.

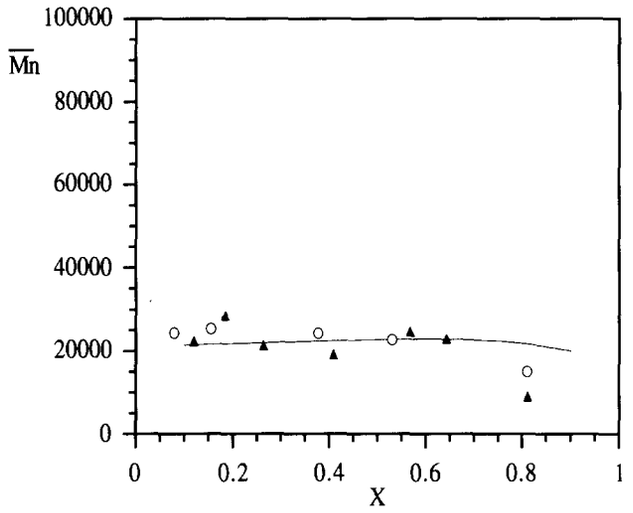

Figure 12 Comparison between experimental and calculated values of $\bar{M}_n$ for the miniemulsion polymerizations initiated by BPO: (—) model calculations; (○) miniemulsion polymerization; (▲) 'classical' miniemulsion polymerization

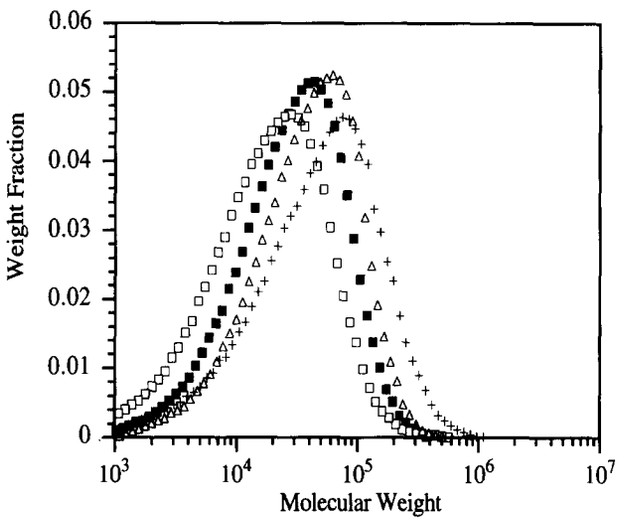

Figure 13 Comparison of the *MWD* of the final samples of the polymerizations initiated by BPO: (■) miniemulsion polymerization; (□) 'classical' miniemulsion polymerization; (△) coagulated fraction of the conventional emulsion polymerization; (+) non-coagulated fraction of the conventional emulsion polymerization

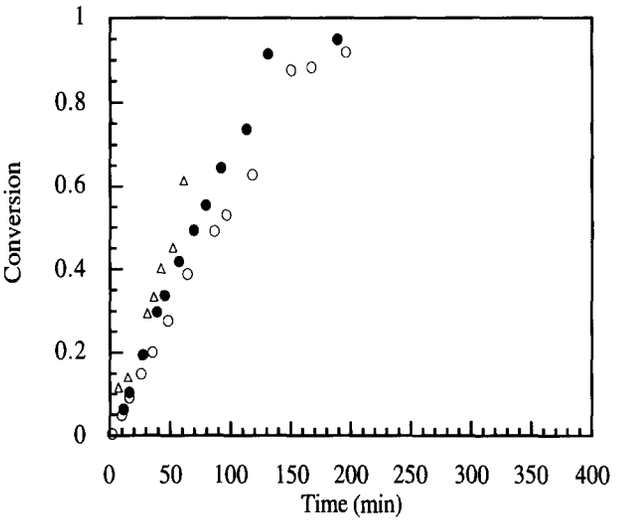

Figure 14 Time evolution of the conversion in the polymerizations initiated by AIBN: (○) miniemulsion polymerization; (●) 'classical' miniemulsion polymerization; (△) conventional emulsion polymerization

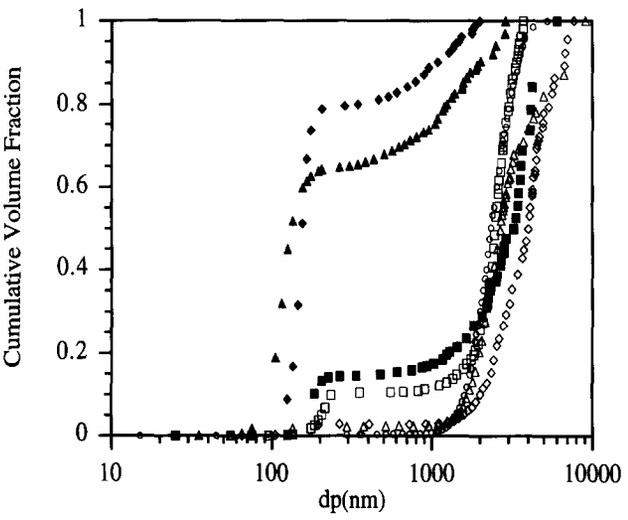

Figure 15 Cumulative particle volume distribution in the miniemulsion polymerizations initiated by AIBN. Miniemulsion polymerization (run 3): (○) $x=0.09$; (△) $x=0.28$; (◇) $x=0.61$; (□) $x=0.88$. 'Classical' miniemulsion polymerization (run 6): (▲) $x=0.34$; (◆) $x=0.64$; (■) $x=0.95$

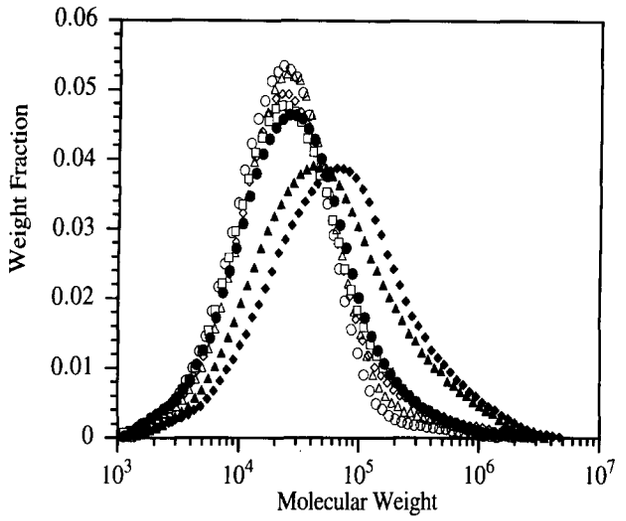

Figure 16 Evolution of the *MWD* in the miniemulsion polymerization initiated by AIBN: (○) $x=0.09$; (△) $x=0.15$; (◇) $x=0.28$; (□) $x=0.49$; (●) $x=0.61$; (▲) $x=0.88$; (◆) $x=0.92$

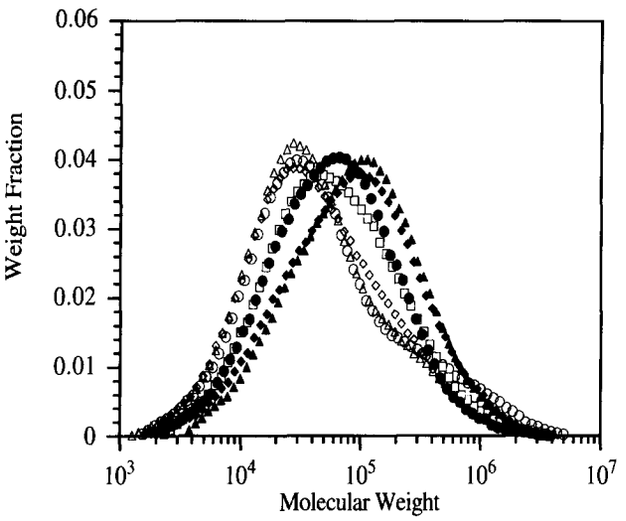

Figure 17 Evolution of the *MWD* during the 'classical' miniemulsion polymerization initiated by AIBN: (○) $x=0.06$; (△) $x=0.19$; (◇) $x=0.30$; (□) $x=0.42$; (●) $x=0.64$; (▲) $x=0.74$; (◆) $x=0.95$

The conventional emulsion polymerization could not be completed because extensive coagulation occurred. Coagulum and latex were separated by filtration, finding that 45 wt% of the polymer was in the coagulum.

Figures 16 and *17* present the evolution of the *MWD* during the miniemulsion processes initiated by AIBN. In both processes, molecular weight was roughly constant at the beginning of the polymerization and sharply increased after $x=0.6$ due to the gel effect. Because of its larger compartmentalization degree, the molecular weights for the 'classical' miniemulsion polymerization (run 6) were higher than those obtained in the miniemulsion polymerization (run 3). *Figure 18* presents a comparison between the *MWD* of the final samples of the polymerizations carried out with AIBN. It can be seen that the molecular weight of the coagulum from the conventional emulsion polymerization, which presumably corresponds to bulk polymerization, is significantly lower than those of the miniemulsion processes. Compartmentalization cannot be claimed as a reason for this difference because *Figure 15* shows that in the miniemulsion polymerization most of the polymer was in large particles ($d_p > 1000$ nm) where the compartmentalization effect is negligible (see *Figure 4*). A speculative reason for the low molecular weights of the coagulum is that a local temperature increase developed in the coagulum due to the low heat transfer coefficient of the polymer–monomer mixture, which makes it difficult to dissipate the heat of polymerization. *Figure 19* presents a comparison between the experimental results and model predictions for the evolution of M_n in the miniemulsion polymerizations initiated by AIBN. It can be seen that the model predictions obtained assuming bulk-like conditions agreed well with those measured in the miniemulsion process but are lower than the ones obtained in the 'classical' miniemulsion polymerization. This further supports the hypothesis that compartmentalization was significant in the 'classical' miniemulsion process.

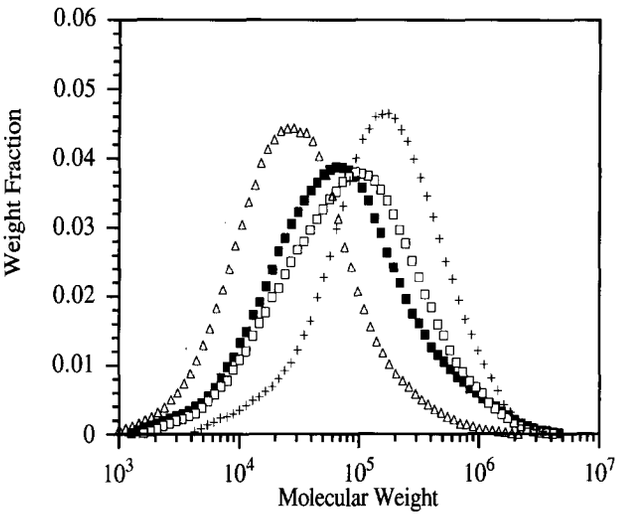

Figure 18 Comparison of the *MWD* of the final samples of the polymerizations initiated by AIBN: (■) miniemulsion polymerization; (□) 'classical' miniemulsion polymerization; (△) coagulated fraction of the conventional emulsion polymerization; (+) non-coagulated fraction of the conventional emulsion polymerization

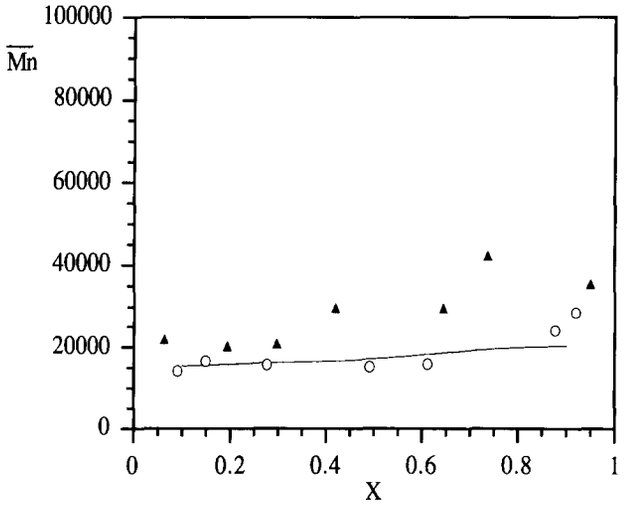

Figure 19 Comparison between experimental and calculated values of $\bar{M}_n$ for the miniemulsion polymerizations initiated by AIBN: (—) model calculations; (○) miniemulsion polymerization; (▲) 'classical' miniemulsion polymerization

CONCLUSIONS

The evolution of the *MWD* in the batch miniemulsion polymerization of styrene initiated by different oil-soluble initiators (LPO, BPO and AIBN) was investigated. When LPO was used, the effect of compartmentalization on *MWD* was negligible and the molecular weights remained roughly constant at the beginning of the polymerization and increased significantly at the end due to the gel effect. These results were analysed by means of a mathematical model. A fairly good agreement between experimental results and model predictions was achieved using values of the parameters from the literature. Compartmentalization was also negligible for the miniemulsion polymerizations initiated by BPO. However, a rather low molecular weight was obtained and, in spite of the conversion–time curves showing a distinct gel effect, the molecular weight decreased during polymerization. According to the model, this decrease was due to chain transfer to the initiator, which counteracted the influence of the gel effect. The molecular weights of the polymer produced through the 'classical' miniemulsion polymerization initiated by AIBN were larger than those corresponding to the miniemulsion polymerization. This difference was due to the fact that, in the 'classical' miniemulsion polymerization, a significant part of the polymer was produced in small particles (where substantial compartmentalization occurred), whereas in the miniemulsion polymerization, most of the polymer was in large particles (negligible compartmentalization).

ACKNOWLEDGEMENT

The financial support by the Excma. Diputación Foral de Gipuzkoa is gratefully appreciated.

REFERENCES

1 Ugelstad, J., El-Aasser, M. S. and Vanderhoff, J. W. *J. Polym. Sci., Polym. Lett. Edn.* 1973, **11**, 503
2 Delgado, J. and El-Aasser, M. S. *Makromol. Chem., Macromol. Symp.* 1990, **31**, 63
3 Unzué, M. J. and Asua, J. M. *J. Polym. Sci.* 1993, **49**, 81
4 Barnette, D. T. and Schork, F. J. *Chem. Eng. Prog.* 1987, **83**, 25
5 Alduncin, J. A., Forcada, J. and Asua, J. M. *Macromolecules* 1994, **27**, 2256
6 Kirk, R. E. and Othmer, D. F. in 'Encyclopedia of Chemical Technology', Vol. 15, Wiley-Interscience, New York, 1978, p. 902
7 Yalkowsky, S. H. and Barnerjee, S. in 'Aqueous Solubility. Methods of Estimation for Organic Compounds', Marcel Dekker, New York, 1992
8 Redington, L. E. *J. Polym. Sci.* 1948, **3**, 503
9 Breintenbach, J. W. and Schindler, A. *Monatsh. Chem.* 1952, **83**, 724
10 Young, L. J. in 'Polymer Handbook' (Eds. J. Brandrup and E. H. Immergut), Wiley, New York, 1974
11 Cheng, S. A. and Jeng, W. F. *Chem. Eng. Sci.* 1978, **33**, 735
12 Gopalan, M. R. and Santhappa, M. *J. Polym. Sci.* 1957, **25**, 333
13 Friis, N. and Hamielec, A. E. in 'Emulsion Polymerization' (Eds. I. Piirma and J. L. Gardon), ACS Symp. Ser. **24**, American Chemical Society, Washington, DC, 1976
14 Asua, J. M., Rodríguez, V. S., Sudol, E. D. and El-Aasser, M. S. *J. Polym. Sci. (A) Polym. Chem.* 1989, **27**, 3569
15 Gardon, J. L. *J. Polym. Sci. (A-1)* 1968, **6**, 643
16 Hui, A. and Hamielec, A. E. *J. Appl. Polym. Sci.* 1972, **16**, 749